

Pseudo-Jahn-Teller Effect and Magnetoelastic Coupling in Spin-Orbit Mott Insulators

Huimei Liu and Giniyat Khaliullin

Max Planck Institute for Solid State Research, Heisenbergstrasse 1, D-70569 Stuttgart, Germany

(Dated: February 7, 2019)

The consequences of the Jahn-Teller (JT) orbital-lattice coupling for magnetism of pseudospin $J_{\text{eff}} = 1/2$ and $J_{\text{eff}} = 0$ compounds are addressed. In the former case, represented by Sr_2IrO_4 , this coupling generates, through the so-called pseudo-JT effect, orthorhombic deformations of a crystal concomitant with magnetic ordering. The orthorhombicity axis is tied to the magnetization and rotates with it under magnetic field. The theory resolves a number of puzzles in Sr_2IrO_4 such as the origin of in-plane magnetic anisotropy and magnon gaps, metamagnetic transition, etc. In $J_{\text{eff}} = 0$ systems, the pseudo-JT effect leads to spin-nematic transition well above magnetic ordering, which may explain the origin of “orbital order” in Ca_2RuO_4 .

Electron-phonon coupling leads to a wide range of phenomena, from Cooper pairing in metals to the Jahn-Teller (JT) effect in Mott insulators. The JT effect, arising from coupling of the orbital degrees of freedom of localized electrons to lattice vibrations (“orbital-lattice coupling”), is a major source driving structural phase transitions. Below the JT structural transition temperature T_{JT} , the orbital fluctuations are quenched, and resulting orbital order dictates the spin-exchange couplings J and magnetic structure below T_m via so-called Goodenough-Kanamori rules [1, 2]. Typically, the JT and magnetic transitions are well separated; a canonical example is LaMnO_3 with $T_{\text{JT}} \sim 800$ K and $T_m \sim 140$ K.

The picture of successive orbital and spin orderings, and associated Goodenough-Kanamori rules that guided spin-orbital physics in transition metal compounds over decades, are based on a spin-orbital separation idea assuming distinct energy scales and excitations in spin and orbital sectors. Recently, materials based on late transition metal ions with strong spin-orbit coupling (SOC) came into focus. In these compounds, spin-orbital separation is no longer at work, and both magnetism and JT physics have to be reformulated in terms of “pseudospins” [1], or “effective spins” J_{eff} [4], corresponding (but not always) to the total angular momentum. While the pseudospin magnetism, especially in $J_{\text{eff}} = 1/2$ systems, is now well understood (see the recent reviews [5–9]), the JT physics in spin-orbit Mott insulators remains largely unexplored. Partially, this is due to the common belief that JT coupling in $J_{\text{eff}} = 1/2$ systems is not essential at all, since it cannot split the Kramers doublet.

In this Letter, we show that JT coupling has in fact a decisive impact on low-energy magnetic properties of $J_{\text{eff}} = 1/2$, and even nominally nonmagnetic $J_{\text{eff}} = 0$, compounds. By virtue of the pseudo-JT effect [10–12], orbital-lattice coupling modulates the spatial shape of the pseudospin wave function and generates new terms in the Hamiltonian, describing the pseudospin-lattice coupling. Albeit weak, these terms lead to the qualitative effects: in the $J_{\text{eff}} = 1/2$ system Sr_2IrO_4 , we predict that they induce the tetragonal-to-orthorhombic structural transition, which turns out to be instrumental for

understanding the magnetic properties of this compound, including metamagnetic behavior, the origin of magnon gaps, etc. In $J_{\text{eff}} = 0$ systems, the JT coupling results in a simultaneous lattice and spin-rotational symmetry breaking transition well above T_m .

Pseudospin-lattice coupling, $J_{\text{eff}} = 1/2$.— While physical ideas are generic to a broad class of spin-orbit Mott insulators [5–9, 13, 14], we focus here on Sr_2IrO_4 , which is of special interest due to its quasi-two-dimensional (2D) antiferromagnetism (AF) [15] and magnon excitations [16] similar to those of La_2CuO_4 [17].

The JT interaction operates in a quadrupolar channel; i.e., it couples lattice deformations ε_γ of certain symmetry γ to the orbital quadrupolar moments Q^γ of valence electrons: $\mathcal{H}_{\text{JT}} \propto g_\gamma \varepsilon_\gamma Q^\gamma$. Through the spin-orbit entanglement, this coupling should generate pseudospin-lattice coupling \mathcal{H}_{s-l} of the same form, with Q^γ replaced by the pseudospin quadrupoles Q_s^γ . As no single-ion quadrupole can be formed out of pseudospin $S = 1/2$, Q_s^γ should involve at least two sites, i.e., bilinear forms $S_i^\alpha S_j^\beta$ of a proper symmetry, suggesting a minimal coupling $\mathcal{H}_{s-l}^{ij} \propto \tilde{g}_\gamma \varepsilon_\gamma Q_s^\gamma(ij)$. Below, we derive this interaction and evaluate the coupling constants \tilde{g}_γ .

We consider the orthorhombic deformations which are common in perovskites. In a tetragonal Sr_2IrO_4 , these are xy and x^2-y^2 type distortions, which we quantify by $\varepsilon_1 = \frac{b-a}{b+a}$ and $\varepsilon_2 = \frac{x-y}{x+y}$, correspondingly, using the coordinate frames of Fig. 1, where a and b axes are rotated by 45° with respect to cubic x and y axes. ε_1 and ε_2 measure elongation of a crystal along b and x directions, respectively. The distortions split t_{2g} level via the JT coupling:

$$\mathcal{H}_{\text{JT}} = g_1 \varepsilon_1 (n_{az} - n_{bz}) + g_2 \varepsilon_2 (n_{xz} - n_{yz}), \quad (1)$$

where $n_{az} = d_{az}^\dagger d_{az}$ and $n_{bz} = d_{bz}^\dagger d_{bz}$ are densities of the $az = \frac{1}{\sqrt{2}}(x-y)z$ and $bz = \frac{1}{\sqrt{2}}(x+y)z$ orbitals. This coupling mixes the Kramers doublets A and B of Ir^{4+} ion (Fig. 1), resulting in the “orthorhombically distorted” pseudospin wave function \tilde{A} :

$$|\tilde{A}_\pm\rangle = \frac{1}{\sqrt{1+|\eta_\pm|^2}} (|A_\pm\rangle + \eta_\pm |B_\mp\rangle), \quad (2)$$

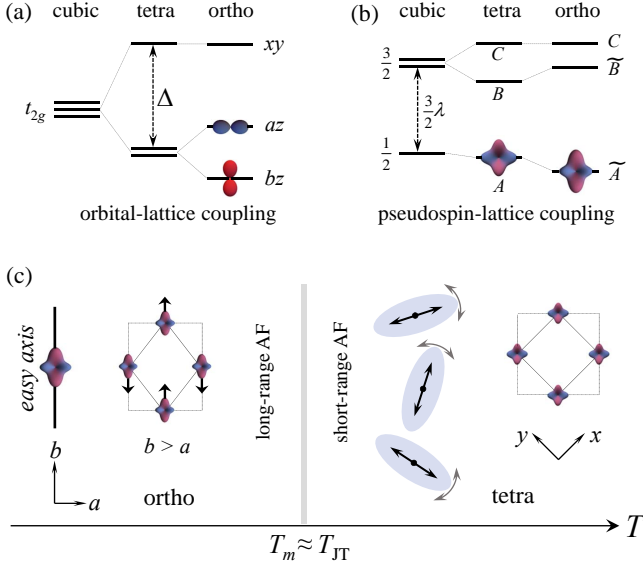


FIG. 1: t_{2g} -hole level structure (a) without and (b) with SOC under cubic, tetragonal, and orthorhombic crystal fields. ($\Delta > 0$ corresponds to the case of Sr_2IrO_4 [18–20]). Elongation of a crystal along the b axis (ε_1 deformation) splits az (blue) and bz (red) orbitals. This enhances the bz component of the ground state wave function \tilde{A} , breaking its tetragonal symmetry (top view; xy orbital is not shown for clarity). (c) Illustration of the magnetoelastic coupling in Sr_2IrO_4 . Above the structural transition at $T_{\text{JT}} \approx T_m$, symmetry is tetragonal on average, but slowly rotating domains of the orthorhombic distortions and quasi-2D magnetism develop. Below T_{JT} , the tetragonal symmetry is broken, selecting the b axis for the moment direction.

where $\eta_{\pm} = \frac{\cos\theta}{E_{BA}}(\pm ig_1\varepsilon_1 + g_2\varepsilon_2)$. The angle θ with $\tan 2\theta = 2\sqrt{2}\lambda/(\lambda + 2\Delta)$ quantifies a tetragonal field Δ relative to SOC constant λ , and $E_{BA} \sim \frac{3}{2}\lambda$ is the energy difference between A and B levels [21]. The “tetragonal”, i.e., unperturbed wave functions $|A_{\pm}\rangle = \sin\theta|0, \pm\frac{1}{2}\rangle - \cos\theta|\pm 1, \mp\frac{1}{2}\rangle$ and $|B_{\pm}\rangle = |\pm 1, \pm\frac{1}{2}\rangle$, in terms of t_{2g} orbital and spin quantum numbers $|l_z, s_z\rangle$.

Next, we inspect how the shape distortions of the ground state wave function \tilde{A} affect the pseudospin interactions. Deformations are assumed to be quasistatic (adiabatic approximation). Projecting the Kugel-Khomskii-type spin-orbital Hamiltonian, Eq. (3.11) of Ref. [1], onto \tilde{A} subspace, we find $\mathcal{H} = \mathcal{H}_s + \mathcal{H}_{s-l}$. \mathcal{H}_s comprises the nearest-neighbor Heisenberg J , Ising J_z , Dzyaloshinskii-Moriya D , and pseudodipolar K terms

$$J\vec{S}_i \cdot \vec{S}_j + J_z S_i^z S_j^z + \vec{D} \cdot [\vec{S}_i \times \vec{S}_j] + K(\vec{S}_i \cdot \vec{r}_{ij})(\vec{S}_j \cdot \vec{r}_{ij}) \quad (3)$$

derived earlier [23], while

$$\mathcal{H}_{s-l}^{ij} = \tilde{g}_1\varepsilon_1(S_i^x S_j^y + S_i^y S_j^x) + \tilde{g}_2\varepsilon_2(S_i^x S_j^x - S_i^y S_j^y) \quad (4)$$

constitutes the (pseudo)spin-lattice interaction that we are looking for [24]. It linearly couples the spin

quadrupoles Q_s^1 and Q_s^2 of xy and $x^2 - y^2$ symmetries to corresponding lattice deformations. In essence, \mathcal{H}_{s-l} is nothing but \mathcal{H}_{JT} “reincarnated” as a spin-lattice coupling in $J_{\text{eff}} = 1/2$ insulator. The coupling constants \tilde{g} are renormalized from g of Eq. 1 to $\tilde{g} = \kappa g$ by $\kappa \simeq \frac{t^2 \sin^2 2\theta J_H}{U E_{BA} U}$, where t , U , and J_H are hopping amplitude, Coulomb repulsion, and Hund’s coupling, respectively. Roughly, we estimate $\kappa \sim 5 \times 10^{-3}$ and hence $\tilde{g} \sim 25$ meV in Sr_2IrO_4 , using $g \sim 5$ eV typical for t_{2g} systems. In $J_{\text{eff}} = 1/2$ compounds based on $4d$ Ru^{3+} and $3d$ Co^{2+} ions, κ and \tilde{g} should increase as $1/\lambda$.

Breaking tetragonal symmetry.— Having derived spin-lattice interaction \mathcal{H}_{s-l} , we discuss now its consequences for low-energy properties of Sr_2IrO_4 . First of all, just as the JT coupling, it should lead to the structural instability as soon as the spin quadrupolar moments Q_s^{γ} develop within the (quasi) long-range ordered magnetic domains. Denoting the staggered moment direction by α , $\vec{n} = S(\cos\alpha, \sin\alpha)$, we find $\langle Q_s^1 \rangle = -S^2 \sin 2\alpha$ and $\langle Q_s^2 \rangle = -S^2 \cos 2\alpha$ per bond. From Eq. (4) and elastic energy $\frac{1}{2}K_{\gamma}\varepsilon_{\gamma}^2$, the spin-lattice induced orthorhombic deformations follow:

$$\langle \varepsilon_1 \rangle = \frac{\Gamma_1}{\tilde{g}_1} \sin 2\alpha, \quad \langle \varepsilon_2 \rangle = \frac{\Gamma_2}{\tilde{g}_2} \cos 2\alpha, \quad (5)$$

where $\Gamma_{\gamma} = 2S^2\tilde{g}_{\gamma}^2/K_{\gamma}$. A mean-field part of \mathcal{H}_{s-l} (4) reads then as follows:

$$\Gamma_1 \sin 2\alpha (S_i^x S_j^y + S_i^y S_j^x) + \Gamma_2 \cos 2\alpha (S_i^x S_j^x - S_i^y S_j^y), \quad (6)$$

with α to be obtained by minimizing the ground state energy E_{α} . Classically, $E_{\alpha} = \text{const} + S^2(\Gamma_1 - \Gamma_2) \cos^2 2\alpha$ [25]. For $\Gamma_1 > \Gamma_2$, E_{α} is minimized at $\alpha = 45^\circ$, which is exactly the case of Sr_2IrO_4 [15, 26]. Our theory predicts then ε_1 -type ($b > a$) orthorhombic distortion, as depicted in Fig. 1(c). This type of distortion is natural for perovskites, as it does not affect the Me-O-Me bond length.

Breaking C_4 symmetry by spin-lattice coupling opens the in-plane magnon gap already on a level of linear spin-wave theory. Equations. 3 and 6 give $\omega_{ab} \simeq 8S\sqrt{J\Gamma_1}$. With $\omega_{ab} \sim 2.1 - 2.4$ meV [27, 28] and $J \sim 100$ meV [16, 29], we evaluate $\Gamma_1 \sim 3$ μeV . Equation. 5 predicts then the spin-lattice induced distortion of the order of $\varepsilon_1 \sim 10^{-4}$ [30]. The twofold C_2 anisotropy of magnetoresistivity [33] and the signatures of orthorhombic distortions [34, 35] in Sr_2IrO_4 find a natural explanation within our theory. Future experiments using, e.g., Larmor diffraction [36] should be able to quantify ε_1 directly. We note also that the deformation induced magnon gap ω_{ab} far exceeds interlayer couplings [37], and should therefore be essential for establishing the magnetic order at high $T_m \sim 240$ K.

To summarize up to now, the combined action of spin-orbit and JT couplings results in the interaction between magnetic quadrupoles and lattice deformation. Dynamically, coupled oscillations of the \vec{n} -moment direction and

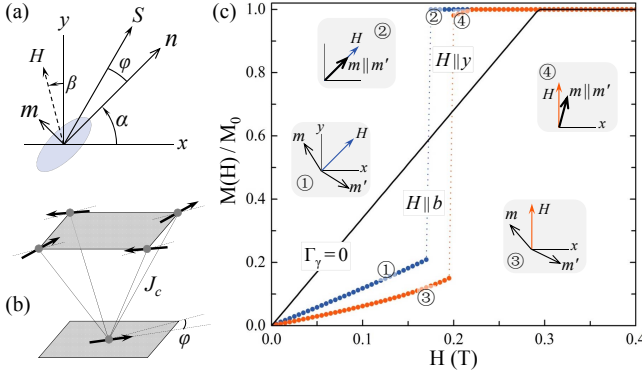


FIG. 2: Schematic of (a) staggered \vec{n} and canted \vec{m} moments, magnetic field H , and spin-lattice induced orthorhombic deformation (shaded ellipse), and (b) interlayer AF coupling J_c between spins. (c) Magnetization curves for a magnetic field applied along the "easy" ($H \parallel b$) and "hard" ($H \parallel y$) axes. While the magnetization $\vec{M} \propto \vec{m} + \vec{m}'$ grows linearly with H when $\Gamma_\gamma = 0$, a metamagnetic transition caused by magnetoelastic coupling is observed at finite Γ_γ (we used $\Gamma_1 = 3 \mu\text{eV}$ and $\Gamma_2 = 0.6\Gamma_1$). Insets depict the mutual orientation of \vec{m} and \vec{m}' moments on different layers at representative points on the $M(H)$ curves.

lattice vibrations (magnetoacoustic effects [38, 39]) are expected; this is an interesting topic for future research. Most importantly, a structural instability is inevitable no matter how large SOC is; this invalidates a common assertion that high tetragonal symmetry of $J_{\text{eff}} = 1/2$ system Sr_2IrO_4 is protected by large SOC.

Metamagnetic transition, in-plane magnon gap.— We discuss now further manifestations of magnetoelastic coupling in Sr_2IrO_4 . Via spin-lattice coupling, the reorientations of moments under external magnetic field will affect lattice deformations. The latter, in turn, modifies the magnetic anisotropy potential. Such feedback effects result in a nonmonotonic behavior of magnetization $M(H)$. In Sr_2IrO_4 , spins are canted by angle $\varphi \simeq D/2J \sim 12^\circ$ [40], see Figs. 2(a) and 2(b). Magnetic field couples to the canted moments \vec{m} . To calculate $M(H)$, we use a simple model in Fig. 2(b) for the interlayer coupling. The total energy E depends now on two angles α and α' , corresponding to the moment directions in different layers, and the field direction β . We find $E(\alpha, \alpha', \beta) = \text{const} + \frac{S}{2}F$, with

$$F = \sin \varphi [h_c \cos(\alpha - \alpha') - h \cos(\alpha - \beta) - h \cos(\alpha' - \beta)] - \frac{S}{2}[\Gamma_1(\sin 2\alpha + \sin 2\alpha')^2 + \Gamma_2(\cos 2\alpha + \cos 2\alpha')^2]. \quad (7)$$

Here, $h = g\mu_B H$, and $h_c = 4J_c S \sin \varphi$ is the interlayer field. Minimization of F gives α and α' as a function of \vec{H} , from which the canted moments \vec{m} and \vec{m}' on different planes and total magnetization \vec{M} follow. The deformations ε_1 and ε_2 are given by Eq. (5), where $\sin 2\alpha$ and $\cos 2\alpha$ replaced now by $\frac{1}{2}(\sin 2\alpha + \sin 2\alpha')$ and

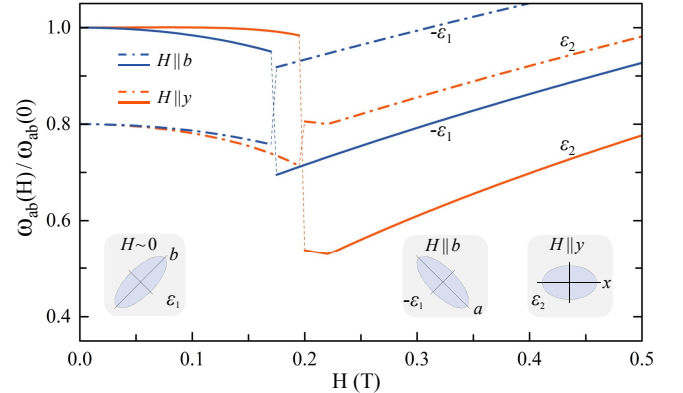


FIG. 3: Magnon gaps as a function of magnetic field along b ([010] in orthorhombic notation, blue) and y ([110], red) directions. Dash-dotted (solid) line corresponds to the in-phase (antiphase) rotations of \vec{m} and \vec{m}' moments. At small H , the distortion is of ε_1 symmetry. At large H , it remains ε_1 type for $H \parallel b$. For $H \parallel y$, the deformation changes from large ε_1 to small ε_2 , resulting in a drop of the anisotropy energy and ω_{ab} . The parameters are as in Fig. 2.

$\frac{1}{2}(\cos 2\alpha + \cos 2\alpha')$, respectively; this implies the field dependence of the deformations (magnetostriction).

Fig. 2(c) shows $M(H)/M_0$ calculated with $h_c = 18 \mu\text{eV} (\simeq 0.16 \text{ T})$. Without spin-lattice coupling, \vec{m} and \vec{m}' gradually rotate towards each other and M grows monotonically. Spin-lattice induced anisotropy results in a metamagnetic transition as observed [15, 26]. At $H = H_{cr}$, \vec{m} and \vec{m}' flip and become parallel. For $\Gamma_1 > \Gamma_2$ as in Sr_2IrO_4 , H_{cr} for easy-axis b is lower than that for hard axis; this result has recently been confirmed experimentally [41]. We note that $M(H)$ near H_{cr} is sensitive to angle β , so the quenched disorder and sample alignment issues should be relevant in the data analysis.

Next, we discuss the in-plane magnon gaps generated by spin-lattice coupling \mathcal{H}_{s-l} . Because of interlayer coupling, there are two different modes. At small fields, $H \ll H_{cr}$, the optical and acoustic mode gaps are $8S\sqrt{J(\Gamma_1 + \frac{\sin \varphi}{4S}h_c)}$ and $8S\sqrt{J\Gamma_1}$, respectively. Above the metamagnetic transition, $H \geq H_{cr}$, we find

$$\omega_{ab}^\pm \simeq 8S\sqrt{J\{\Gamma(\alpha) + \frac{\sin \varphi}{8S}[h \cos(\alpha - \beta) - h_c \pm h_c]\}}. \quad (8)$$

Here, $\Gamma(\alpha) = \Gamma_1 \sin^2 2\alpha + \Gamma_2 \cos^2 2\alpha$, and α follows from $2S(\Gamma_1 - \Gamma_2) \sin 4\alpha = h \sin \varphi \sin(\alpha - \beta)$. For $H \parallel b$, this gives $\alpha = \beta$ ($= -\frac{\pi}{4}$) and $\Gamma(\alpha) = \Gamma_1$. For \vec{H} along y axis, $\alpha \sim \beta$ ($= 0$) and thus $\Gamma(\alpha) \sim \Gamma_2$; this implies weak distortion ε_2 and smaller magnon gap. The main message is that the magnon gaps become strongly dependent on the field direction, as shown in Fig. 3. The above equations should help to quantify Γ_1 and Γ_2 from experiments. The results in Fig. 3 are qualitatively consistent with the recent Raman data [27]; a detailed analysis would require

a derivation of the Raman matrix elements necessary for the mode assignment.

Via the magnetoelastic coupling, quasi-2D AF correlations above T_m [29, 42] should lead to slowly fluctuating lattice deformations (see Fig. 1) which, in turn, will affect phonon dynamics. Indeed, strong Fano anomalies of phonons have been observed in Sr_2IrO_4 [43].

Spin-nematic order in $J_{\text{eff}} = 0$ systems.— Finally, we move to pseudospin $J_{\text{eff}} = 0$ case, and show that, despite having neither orbital nor spin degeneracy, the JT coupling is relevant even here. In general, the $J_{\text{eff}} = 0$ compounds are of interest because they host “excitonic” magnetism [44] - magnetic order via condensation of spin-orbit $J_{\text{eff}} = 0 \rightarrow 1$ excitations. The expected non-Heisenberg-type magnon and amplitude (Higgs) modes have been observed in Ca_2RuO_4 [45, 46]. Also, $J_{\text{eff}} = 0$ systems illustrate well the interplay between three “grand forces” in Mott insulators - the JT coupling, spin-orbital exchange interaction, and spin-orbit coupling [1].

As a toy model, we consider 2D square lattice of $J_{\text{eff}} = 0$ ions (e.g., d^4 Ru^{4+}) in an octahedral field. The t_{2g}^4 orbital configuration is subject to the JT effect; however, it is opposed by SOC that favors spin-orbit singlet $J_{\text{eff}} = 0$ instead [44, 47]. This competition can be resolved by mixing the $J_{\text{eff}} = 0$ wave function with the excited $J_{\text{eff}} = 1$ states, by virtue of spin-orbital exchange interactions. Since $J_{\text{eff}} = 1$ level hosts a quadrupolar moment, the ground state becomes JT active, and the phase transition, breaking simultaneously the lattice and spin-rotational symmetries, may develop. In essence, this is the “spin nematic” phase discussed in the context of large J_{eff} systems [48], but with the quadrupolar order parameter depending now on the $J_{\text{eff}} = 1$ fraction in the condensate.

A minimal model for d^4 system can be cast in terms of bosons $\mathbf{T} = (T_x, T_y, T_z)$, describing excitations from the ground state $J_{\text{eff}} = 0$ singlet to $J_{\text{eff}} = 1$ triplet. The spin-orbit λ and exchange $J \simeq 4t^2/U$ couplings read, in a cubic limit, as follows [44]:

$$\mathcal{H}_{\lambda, J} = \lambda \sum_i n_i^T + J \sum_{\langle ij \rangle} \frac{1}{4} (\mathbf{T}_i^\dagger \cdot \mathbf{T}_j - \mathbf{T}_i \cdot \mathbf{T}_j + H.c.), \quad (9)$$

where $n^T = n_x^T + n_y^T + n_z^T$ and $n_x^T = T_x^\dagger T_x$, etc. The T bosons are subject to “hard-core” constraint $n_i^T \leq 1$ which we treat on a mean-field level [2, 3, 24].

We consider now a tetragonal distortion $\varepsilon = \frac{x+y-2z}{x+y+z}$ of RuO_6 octahedra. The JT coupling splits the xy and xz/yz orbital levels by $g\varepsilon$: $\mathcal{H}_{\text{JT}} = g\varepsilon \frac{1}{3} (n_{zx} + n_{yz} - 2n_{xy})$. This coupling modifies a single-ion level structure of Ru^{4+} as shown in Fig. 4(a), such that $J_{\text{eff}} = 1$ triplet splits into $T_{x/y}$ doublet and T_z singlet by $\Delta_z(\delta) = (\delta + \sqrt{1 + \delta^2} - 1)\lambda$, where $\delta = g\varepsilon/2\lambda$. As a result, the spin gap reduces from λ to $E(\delta) = (\frac{1}{2} + \sqrt{\frac{9}{4} - \delta + \delta^2} - \sqrt{1 + \delta^2})\lambda$. At the critical value of $E(\delta) \sim J$, the $T_{x/y}$ doublet condenses, forming a ground state with finite quadrupole

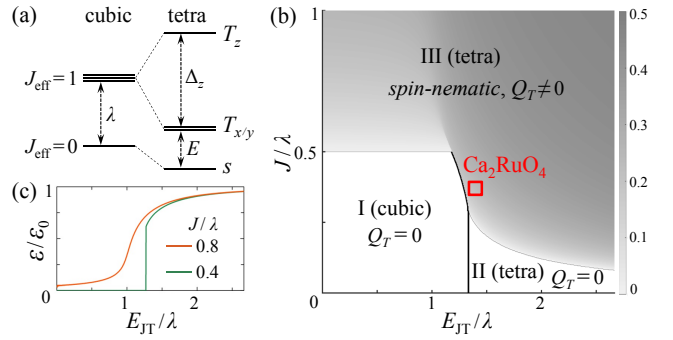


FIG. 4: (a) Singlet-triplet level structure under tetragonal distortion. (b) Phase diagram of $J_{\text{eff}} = 0$ system. Small J area contains two nonmagnetic phases separated by a first order transition (thick line). In phase I, the JT effect is fully suppressed, while phase II is tetragonally distorted. As J increases, the exchange interactions promote condensation of the $T_{x/y}$ states, forming spin-nematic phase with nonzero Q_T moment (quantified by color intensity) and XY -type magnetism. (c) Lattice distortion ε relative to its value ε_0 at $\lambda = 0$ for different J couplings.

moment $Q_T = n_x^T + n_y^T - 2n_z^T$. While the cubic symmetry may be broken at finite temperature T_{JT} , long-range magnetic order is delayed due to XY -type phase fluctuations; therefore, T_m and T_{JT} are separated in quasi-2D $J_{\text{eff}} = 0$ systems. We think that the “orbital order” in Ca_2RuO_4 near 260 K [51], well above T_m , is in fact the JT driven spin-nematic order. The observed XY -type magnons [45] further support the picture of spin-orbit entangled $T_{x/y}$ condensate.

A mean-field phase diagram of $\mathcal{H}_{\lambda, J} + \mathcal{H}_{\text{JT}}$, supplemented by the elastic energy $\frac{1}{2}K\varepsilon^2$, is shown in Fig. 4(b) as a function of J/λ and E_{JT}/λ . $E_{\text{JT}} = \Delta/3$ is the JT stabilization energy, where $\Delta = \frac{2g^2}{3K}$ is the t_{2g} orbital splitting at $\lambda = 0$. At small J and E_{JT} , SOC imposes the $J_{\text{eff}} = 0$ phase I; at large E_{JT} , it gives way to the JT-distorted nonmagnetic phase II with finite spin-gap E . In phase III, stabilized by a cooperative action of the exchange and JT couplings, XY -type magnetic condensate is formed, which, in turn, helps to recover the JT distortion [see Fig. 4(c)].

Interestingly, the observed magnon bandwidth $\sim 2J \sim 50$ meV [45] and ratio $\Delta/2\lambda \sim 2$ [52, 53] locate Ca_2RuO_4 in the critical area of the phase diagram [see Fig. 4(b)]. This suggests that an unusual magnetism [45, 46] and extreme sensitivity of Ca_2RuO_4 to external perturbations [54, 55] are caused by frustration among the JT, spin-orbit, and exchange interactions, further boosted by its proximity to metal-insulator transition.

To conclude, in contrast to the common wisdom, the JT coupling remains an essential part of the low-energy physics in spin-orbit $J_{\text{eff}} = 1/2$, and even $J_{\text{eff}} = 0$, Mott insulators. Converted into pseudospin-lattice coupling via spin-orbit entanglement, it leads to the structural

transitions and magnetoelastic effects. We have shown that the JT coupling resolves hitherto unexplained puzzles of $J_{\text{eff}} = 1/2$ Sr₂IrO₄, and is essential for the phase behavior of $J_{\text{eff}} = 0$ Ca₂RuO₄. This leads us to believe that pseudospin-lattice coupling should be generic to a broad class of spin-orbit J_{eff} compounds, including the Kitaev-model materials of high current interest [5–8]. In the latter, the pseudospins are highly frustrated, and their coupling to lattice may lead to more radical effects than in conventional, unfrustrated magnets like Sr₂IrO₄.

We thank B. J. Kim, J. Porras, J. Bertinshaw, B. Keimer, J. Chaloupka, and O. P. Sushkov for discussions. We acknowledge support by the European Research Council under Advanced Grant No. 669550 (Com4Com).

[1] J. B. Goodenough, *Magnetism and the Chemical Bond* (Interscience Publisher, New York, 1963).

[2] K. I. Kugel and D. I. Khomskii, Sov. Phys. Usp. **25**, 231 (1982).

[3] G. Khaliullin, Prog. Theor. Phys. Suppl. **160**, 155 (2005).

[4] B. J. Kim, H. Jin, S. J. Moon, J.-Y. Kim, B.-G. Park, C. S. Leem, J. Yu, T. W. Noh, C. Kim, S.-J. Oh, J.-H. Park, V. Durairaj, G. Cao, and E. Rotenberg, Phys. Rev. Lett. **101**, 076402 (2008).

[5] J. G. Rau, E. K.-H. Lee, and H.-Y. Kee, Annu. Rev. Condens. Matter Phys. **7**, 195 (2016).

[6] S. M. Winter, A. A. Tsirlin, M. Daghofer, J. van den Brink, Y. Singh, P. Gegenwart, and R. Valentí, J. Phys.: Condens. Matter **29**, 493002 (2017).

[7] S. Trebst, *Lecture notes of the 48th IFF spring school topological matter* (2017) arXiv:1701.07056.

[8] M. Hermanns, I. Kimchi, and J. Knolle, Annu. Rev. Condens. Matter Phys. **9**, 17 (2018).

[9] J. Bertinshaw, Y. K. Kim, G. Khaliullin, and B.J. Kim. Annu. Rev. Condens. Matter Phys. **10**, 315 (2019).

[10] The pseudo-JT effect is an extension of the JT effect to systems with orbital-singlet ground states; it operates through the mixing of the ground and excited states under the nuclear displacements [11, 12].

[11] I. B. Bersuker, Chem. Rev. **113**, 1351 (2013).

[12] I. B. Bersuker, *The Jahn-Teller Effect* (Cambridge University Press, Cambridge, 2006).

[13] H. Liu and G. Khaliullin, Phys. Rev. B **97**, 014407 (2018).

[14] R. Sano, Y. Kato, and Y. Motome, Phys. Rev. B **97**, 014408 (2018).

[15] B. J. Kim, H. Ohsumi, T. Komesu, S. Sakai, T. Morita, H. Takagi, and T. Arima, Science **323**, 1329 (2009).

[16] J. Kim, D. Casa, M. H. Upton, T. Gog, Y.-J. Kim, J. F. Mitchell, M. van Veenendaal, M. Daghofer, J. van den Brink, G. Khaliullin, and B. J. Kim, Phys. Rev. Lett. **108**, 177003 (2012).

[17] See Ref. [9] for an extensive discussion of the analogy between iridates and cuprates.

[18] J. Kim, M. Daghofer, A. H. Said, T. Gog, J. van den Brink, G. Khaliullin, and B. J. Kim, Nat. Commun. **5**, 4453 (2014).

[19] S. Fujiyama, H. Ohsumi, K. Ohashi, D. Hirai, B. J. Kim, T. Arima, M. Takata, and H. Takagi, Phys. Rev. Lett. **112**, 016405 (2014).

[20] N. A. Bogdanov, V. M. Katukuri, J. Romhányi, V. Yushankhai, V. Kataev, B. Büchner, J. van den Brink, and L. Hozoi, Nat. Commun. **6**, 7306 (2015).

[21] In a solid, spin-orbit excitation energy E_{BA} depends on momentum [18, 22]; we neglect this effect here.

[22] E. M. Plotnikova, M. Daghofer, J. van den Brink, and K. Wohlfeld, Phys. Rev. Lett. **116**, 106401 (2016).

[23] G. Jackeli and G. Khaliullin, Phys. Rev. Lett. **102**, 017205 (2009).

[24] See Supplemental Material for details of the derivation of Eq. 4 and a mean-field treatment of $J_{\text{eff}} = 0$ model.

[25] On a classical level, i.e., neglecting quantum corrections from magnon-magnon interactions, in-plane anisotropy is solely due to spin-lattice coupling.

[26] G. Cao, J. Bolivar, S. McCall, J. E. Crow, and R. P. Guertin, Phys. Rev. B **57**, R11039 (1998).

[27] Y. Gim, A. Sethi, Q. Zhao, J. F. Mitchell, G. Cao, and S. L. Cooper, Phys. Rev. B **93**, 024405 (2016).

[28] H. Gretarsson, J. Sauceda, N. H. Sung, M. Höppner, M. Minola, B. J. Kim, B. Keimer, and M. Le Tacon, Phys. Rev. B **96**, 115138 (2017).

[29] S. Fujiyama, H. Ohsumi, T. Komesu, J. Matsuno, B. J. Kim, M. Takata, T. Arima, and H. Takagi, Phys. Rev. Lett. **108**, 247212 (2012).

[30] We recall that $\varepsilon \propto \tilde{g} \propto 1/\lambda$. In pseudospin-1/2 Co²⁺ compounds, where λ is one order of value smaller than in iridates, magnetic order induced distortions should be of the order of 10⁻³, as indeed observed [31, 32].

[31] A. Okazaki and Y. Suemune, J. Phys. Soc. Jpn. **16**, 671 (1961).

[32] N. C. Tombs and H. P. Rooksby, Nature **165**, 442 (1950).

[33] C. Wang, H. Seinige, G. Cao, J.-S. Zhou, J. B. Goodenough, and M. Tsoi, J. Appl. Phys. **117**, 17A310 (2015).

[34] C. Dhital, T. Hogan, Z. Yamani, C. de la Cruz, X. Chen, S. Khadka, Z. Ren, and S. D. Wilson, Phys. Rev. B **87**, 144405 (2013).

[35] F. Ye, S. Chi, B. C. Chakoumakos, J. A. Fernandez-Baca, T. Qi, and G. Cao, Phys. Rev. B **87**, 140406(R) (2013).

[36] B. Náfrádi, T. Keller, F. Hardy, C. Meingast, A. Erb, and B. Keimer, Phys. Rev. Lett. **116**, 047001 (2016).

[37] T. Takayama, A. Matsumoto, G. Jackeli, and H. Takagi, Phys. Rev. B **94**, 224420 (2016).

[38] C. Kittel, Phys. Rev. **110**, 836 (1958).

[39] E. A. Turov and V. G. Shavrov, Sov. Phys. Usp. **26**, 593 (1983).

[40] S. Boseggia, H. C. Walker, J. Vale, R. Springell, Z. Feng, R. S. Perry, M. Moretti Sala, H. M. Rønnow, S. P. Collins, and D. F. McMorrow, J. Phys.: Condens. Matter **25**, 422202 (2013).

[41] J. Porras, J. Bertinshaw, H. Liu, G. Khaliullin, N. H. Sung, J.-W. Kim, S. Francoual, P. Steffens, G. Deng, M. Moretti Sala, A. Effimenco, A. Said, D. Casa, X. Huang, T. Gog, J. Kim, B. Keimer, and B. J. Kim, arXiv:1808.06920.

[42] J. G. Vale, S. Boseggia, H. C. Walker, R. Springell, Z. Feng, E. C. Hunter, R. S. Perry, D. Prabhakaran, A. T. Boothroyd, S. P. Collins, H. M. Rønnow, and D. F. McMorrow, Phys. Rev. B **92**, 020406(R) (2015).

[43] H. Gretarsson, N. H. Sung, M. Höppner, B. J. Kim, B. Keimer, and M. Le Tacon, Phys. Rev. Lett. **116**, 136401 (2016).

[44] G. Khaliullin, Phys. Rev. Lett. **111**, 197201 (2013).

- [45] A. Jain, M. Krautloher, J. Porras, G. H. Ryu, D. P. Chen, D. L. Abernathy, J. T. Park, A. Ivanov, J. Chaloupka, G. Khaliullin, B. Keimer, and B. J. Kim, *Nat. Phys.* **13**, 633 (2017).
- [46] S. M. Souliou, J. Chaloupka, G. Khaliullin, G. Ryu, A. Jain, B. J. Kim, M. Le Tacon, and B. Keimer, *Phys. Rev. Lett.* **119**, 067201 (2017).
- [47] O. N. Meetei, W. S. Cole, M. Randeria, and N. Trivedi, *Phys. Rev. B* **91**, 054412 (2015).
- [48] G. Chen, R. Pereira, and L. Balents, *Phys. Rev. B* **82**, 174440 (2010).
- [49] T. Sommer, M. Vojta, and K. W. Becker, *Eur. Phys. J. B* **23**, 329 (2001).
- [50] M. Matsumoto, B. Normand, T. M. Rice, and M. Sigrist, *Phys. Rev. B* **69**, 054423 (2004).
- [51] I. Zegkinoglou, J. Strempfer, C. S. Nelson, J. P. Hill, J. Chakhalian, C. Bernhard, J. C. Lang, G. Srager, H. Fukazawa, S. Nakatsuji, Y. Maeno, and B. Keimer, *Phys. Rev. Lett.* **95**, 136401 (2005).
- [52] L. Das, F. Forte, R. Fittipaldi, C. G. Fatuzzo, V. Granata, O. Ivashko, M. Horio, F. Schindler, M. Dantz, Yi Tseng, D. E. McNally, H. M. Rønnow, W. Wan, N. B. Christensen, J. Pelliciari, P. Olalde-Velasco, N. Kikugawa, T. Neupert, A. Vecchione, T. Schmitt, M. Cuoco, and J. Chang, *Phys. Rev. X* **8**, 011048 (2018).
- [53] H. Gretarsson, H. Suzuki, H. Kim, K. Ueda, M. Krautloher, B. J. Kim, H. Yavaş, G. Khaliullin, and B. Keimer, unpublished.
- [54] C. Sow, S. Yonezawa, S. Kitamura, T. Oka, Kazuhiko Kuroki, F. Nakamura, and Y. Maeno, *Science* **358**, 1084 (2017).
- [55] F. Nakamura, M. Sakaki, Y. Yamanaka, S. Tamaru, T. Suzuki, and Y. Maeno, *Sci. Rep.* **3**, 2536 (2013).

Supplemental Material for Pseudo Jahn-Teller Effect and Magnetoelastic Coupling in Spin-Orbit Mott Insulators

A. Derivation of pseudospin-lattice coupling Hamiltonian \mathcal{H}_{s-1}

For t_{2g} orbital system with spin $s = 1/2$ (single-hole d^5 or single-electron d^1 case), Kugel-Khomskii type spin-orbital exchange in a perovskite lattice can be written as [1]:

$$\begin{aligned} \mathcal{H}_{ij}^{(\gamma)} = & \frac{2t^2}{E_1} (\vec{s}_i \cdot \vec{s}_j + \frac{3}{4}) \left(\mathcal{O}_{ij}^{(\gamma)} - \frac{1}{2} n_i^{(\gamma)} - \frac{1}{2} n_j^{(\gamma)} \right) \\ & + \frac{2t^2}{E_2} (\vec{s}_i \cdot \vec{s}_j - \frac{1}{4}) \left(\mathcal{O}_{ij}^{(\gamma)} + \frac{1}{2} n_i^{(\gamma)} + \frac{1}{2} n_j^{(\gamma)} \right) \\ & + \left(\frac{2t^2}{E_3} - \frac{2t^2}{E_2} \right) (\vec{s}_i \cdot \vec{s}_j - \frac{1}{4}) \frac{2}{3} \mathcal{P}_{ij}^{(\gamma)}. \end{aligned} \quad (S1)$$

Here, t is the nearest-neighbor hopping amplitude between t_{2g} orbitals, $E_1 = U - 3J_H$, $E_2 = U - J_H$, $E_3 = U + 2J_H$, where U and J_H are Coulomb and Hund's interactions, respectively. The orbital operators $\mathcal{O}_{ij}^{(\gamma)}$, $\mathcal{P}_{ij}^{(\gamma)}$, and $n_i^{(\gamma)}$ depend on \vec{r}_{ij} -bond direction γ . In systems with strong SOC, it is convenient to represent these operators in terms of orbital angular momentum operators $l_{x,y,z}$ of t_{2g} level. For $\gamma = x$, we have

$$\begin{aligned} \mathcal{O}_{ij}^{(x)} &= [(1 - l_y^2)_i (1 - l_y^2)_j + (l_y l_z)_i (l_z l_y)_j] + [y \leftrightarrow z], \\ \mathcal{P}_{ij}^{(x)} &= [(1 - l_y^2)_i (1 - l_y^2)_j + (l_y l_z)_i (l_y l_z)_j] + [y \leftrightarrow z], \\ n^{(x)} &= l_x^2, \end{aligned} \quad (S2)$$

while the corresponding expressions for $\gamma = y$ bond follow from symmetry.

Next, we project the Hamiltonian of Eq. S1 onto pseudospin-1/2 subspace defined by wavefunctions $|\tilde{A}_\pm\rangle$ (Eq. 2 in the main text). In terms of orbital and spin quantum numbers $|l_z, s_z\rangle$, they read as follows:

$$\begin{aligned} |\tilde{A}_+\rangle &= \frac{1}{\sqrt{1+|\eta_+|^2}} (\sin \theta |0, +\frac{1}{2}\rangle - \cos \theta |+1, -\frac{1}{2}\rangle + \eta_+ | -1, -\frac{1}{2}\rangle), \\ |\tilde{A}_-\rangle &= \frac{1}{\sqrt{1+|\eta_-|^2}} (\sin \theta |0, -\frac{1}{2}\rangle - \cos \theta |-1, +\frac{1}{2}\rangle + \eta_- | +1, +\frac{1}{2}\rangle). \end{aligned} \quad (S3)$$

We recall $\eta_\pm = \frac{\cos \theta}{E_{BA}} (\pm i g_1 \varepsilon_1 + g_2 \varepsilon_2)$. The pseudospin-lattice coupling \mathcal{H}_{s-1} that we are looking for will be generated by the η_\pm -corrections to $|\tilde{A}_\pm\rangle$.

To project Eq. S1 onto pseudospin $S = 1/2$ sector, one has to calculate the matrix elements of various combinations of spin s_α and orbital l_α operators between $|\tilde{A}_\pm\rangle$ states, and express them via pseudospin $S = 1/2$. For example,

$$\begin{aligned} \langle \tilde{A}_+ | s^+ | \tilde{A}_+ \rangle &= 0, & \langle \tilde{A}_+ | s^+ | \tilde{A}_- \rangle &= \sin^2 \theta, \\ \langle \tilde{A}_- | s^+ | \tilde{A}_+ \rangle &= -2\eta_+ \cos \theta, & \langle \tilde{A}_- | s^+ | \tilde{A}_- \rangle &= 0, \end{aligned} \quad (S4)$$

to first order in η_\pm . Thus, $s^+ = \sin^2 \theta S^+ - 2\eta_+ \cos \theta S^-$. Along the same lines, one obtains the other operators that enter in Eq. S1 and contain η_\pm -terms of interest:

$$\begin{aligned} s^+ l_x^2 &= \sin^2 \theta S^+ + \frac{1}{2} \cos^2 \theta S^- - \eta_+ \cos \theta S^-, \\ s^+ l_z^2 &= -2\eta_+ \cos \theta S^-, \\ l_z l_x &= \frac{\sin \theta}{\sqrt{2}} [(\cos \theta + \eta_+) S^- - (\cos \theta + \eta_-) S^+], \\ s^z l_z l_x &= \frac{\sin \theta}{2\sqrt{2}} [(\cos \theta + \eta_+) S^- + (\cos \theta + \eta_-) S^+]. \end{aligned} \quad (S5)$$

Collecting all the terms $\propto \eta_\pm$, we find the pseudospin-lattice coupling [Eq. (4) of the main text]:

$$\mathcal{H}_{s-1}^{ij} = \tilde{g}_1 \varepsilon_1 (S_i^x S_j^y + S_i^y S_j^x) + \tilde{g}_2 \varepsilon_2 (S_i^x S_j^x - S_i^y S_j^y), \quad (S6)$$

where $\tilde{g} = \kappa g$ and $\kappa \simeq \frac{t^2}{U} \frac{\sin^2 2\theta}{E_{BA}} \frac{J_H}{U}$ (to first order in Hund's coupling). In principle, the form of this Hamiltonian can be inferred from the symmetry considerations (see discussion in the main text).

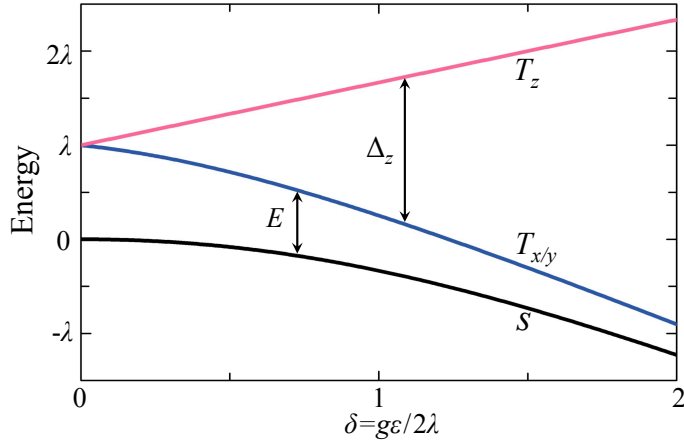


FIG. S1: The energy levels of Ru^{4+} ion under a combined action of spin-orbit coupling λ and Jahn-Teller field $g\varepsilon$ of a tetragonal symmetry. Distance E from a ground state singlet s (black) to $T_{x/y}$ doublet (blue) defines the spin gap to be overcome by the exchange field J . Above a critical value $J_{cr} \sim E/2$, the $T_{x/y}$ bosons condense, while upper level T_z (red) remains unpopulated.

B. Mean-field ground state of $J_{\text{eff}} = 0$ model under tetragonal field

A standard way of handling a hard-core constraint $n_i^T \leq 1$ in singlet-triplet models (see, e.g., Refs. [2, 3]) is to represent T_α -boson via the singlet s and triplet t_α particles: $T_{i,\alpha}^\dagger \Rightarrow t_{i,\alpha}^\dagger s_i$. In this representation, $T_{i,\alpha}^\dagger T_{i,\alpha} = t_{i,\alpha}^\dagger t_{i,\alpha}$, while $T_{i,\alpha}^\dagger T_{j,\alpha} = s_j^\dagger s_i t_{i,\alpha}^\dagger t_{j,\alpha}$. A particle number constraint $s_i^\dagger s_i + \sum_\alpha t_{i,\alpha}^\dagger t_{i,\alpha} = 1$ is implied. On a mean-field level, a singlet amplitude s is replaced by its classical average, $s_i \approx \sqrt{1 - n}$, where $n = \sum_\alpha \langle t_{i,\alpha}^\dagger t_{i,\alpha} \rangle$, resulting in Gutzwiller-type renormalization of the intersite terms $T_{i,\alpha}^\dagger T_{j,\alpha} \approx (1 - n) t_{i,\alpha}^\dagger t_{j,\alpha}$ in the exchange J -Hamiltonian.

Evaluation of a mean-field ground state energy is then straightforward. One first obtains a single-ion multiplets (see Fig. S1), quantified by the lowest singlet s -level at energy

$$E_s(\delta) = \left(\frac{3}{2} - \frac{\delta}{3} - \sqrt{\frac{9}{4} - \delta + \delta^2} \right) \lambda, \quad (\text{S7})$$

a distance to the xy -doublet

$$E(\delta) = \left(\frac{1}{2} + \sqrt{\frac{9}{4} - \delta + \delta^2} - \sqrt{1 + \delta^2} \right) \lambda, \quad (\text{S8})$$

and splitting of a triplet level by $\Delta_z(\delta) = (\delta + \sqrt{1 + \delta^2} - 1)\lambda$, where $\delta = g\varepsilon/2\lambda$. On a classical level, the high energy T_z state is irrelevant, and the exchange interactions induce a condensation of $T_{x/y}$ -type bosons, forming a magnetic quadrupolar moment $Q_T = n_x^T + n_y^T - 2n_z^T$ in the ground state. The value of Q_T and tetragonal distortion ε are obtained by minimizing the total energy including spin-orbit and Jahn-Teller couplings, exchange interactions, and elastic energy:

$$E_{\text{total}} = -2JQ_T^2(\delta) + E_s(\delta) + \frac{1}{2}K\varepsilon^2, \quad (\text{S9})$$

where

$$Q_T(\delta) = \frac{1}{2} \left[1 - \frac{E(\delta)}{2J} \right]. \quad (\text{S10})$$

A numerical analysis of the above equations results in a phase diagram shown in Fig. 4(b) of the main text. The main effect of JT coupling is to reduce spin-orbit coupling induced gap λ to a smaller value of $E(\delta)$, promoting thereby XY -type magnetic condensate.

- [2] T. Sommer, M. Vojta, and K.W. Becker, Eur. Phys. J. B **23**, 329 (2001).
- [3] M. Matsumoto, B. Normand, T. M. Rice, and M. Sigrist, Phys. Rev. B **69**, 054423 (2004).